COMPENSATION OF SECOND-ORDER RANDOM RESONANCES IN THE J-PARC RCS

K. Kojima*, H. Harada, M. Chimura, P. K. Saha
Japan Atomic Energy Agency, JAEA, Tokai, Japan

Abstract

In the Japan Proton Accelerator Research Complex (J-PARC) 3-GeV rapid cycling synchrotron, the shift in the operating point to a higher tune side leads to an increase in the beam loss due to several random resonances excited by the lattice imperfections. To mitigate the resonance-induced beam loss and further enhance the tunability of the operating point, we studied compensating for horizontal half-integer resonance just above the current operating point. A precise half-integer resonance compensation was achieved at the early stage of acceleration by adding trim quadrupole magnets in previous studies. However, the time-dependent component of the lattice imperfections, which is assumed to mainly come from the error field of the main quadrupole magnets, was not evaluated and should deteriorate the resonance compensation during the latter part of the acceleration. We developed a new method for controlling the timing at which the beam approaches the resonance by adjusting the momentum offset and chromaticity-induced tune shift, and experimentally determined the time-dependent component of the lattice imperfections. An analysis based on the resonance driving terms was used to evaluate the optimal resonance compensation for the entire acceleration period.

INTRODUCTION

Figure 1 shows a schematic layout of a 3 GeV rapid cycling synchrotron (RCS) of the Japan Proton Accelerator Research Complex (J-PARC) [1]. The RCS has a three-fold symmetric lattice comprising arc and dispersion-free straight sections. Six trim quadrupole magnets named QDTs are equipped with the RCS at both ends of the straight sections and can be excited individually. The RCS serves as the driver for a material and life science facilities (MLF) as well as the injector for a main ring synchrotron (MR) and provides a 3 GeV proton beam at a repetition ratio of 25 Hz.

In the early stage of acceleration, the space charge force plays a crucial role and pushes the beam toward the lower tune region, as shown in Fig. 2. Although RCS delivers 1 MW beam with a very fractional beam loss, the beam power ramp-up aiming at over 1.5 MW output beam power definitely enhances the space charge force and leads to overlapping of the beam with the structure resonances $\nu_x = 6$ and $\nu_y = 6$ [2–5]. To avoid a beam overlap on the structure resonance, we attempted to compensate for the half-integer resonance $2\nu_x = 13$ located just above the current operating point $(\nu_x, \nu_y) = (6.46, 6.36)$. In previous studies, we successfully demonstrated the half-integer resonance compensation using an additional field generated by the QDTs

* kunihiro.kojima@j-parc.jp

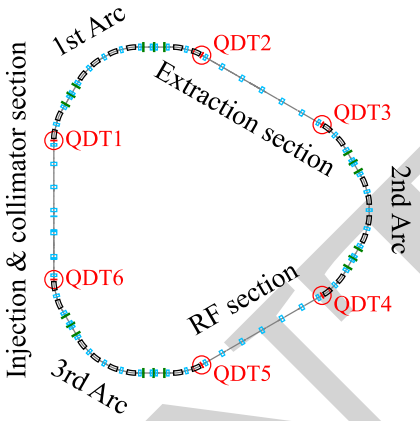

Figure 1: Schematic layout of the RCS. The positions of 6 trim quadrupole magnets named QDT are indicated with red circles.

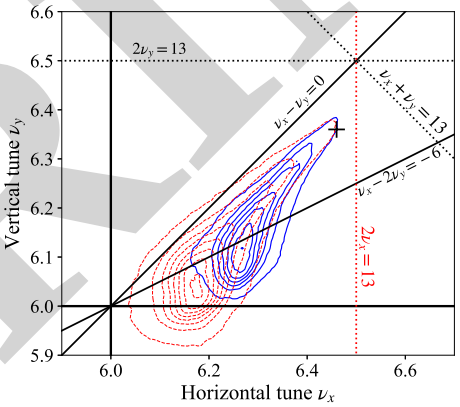

Figure 2: Red curve and blue curve represent the tune footprints of the beam for MLF immediately after injection, corresponding to the output beam powers of 1.5 MW and 1.0 MW, respectively. Structure and random resonances are indicated with solid and dotted lines, respectively. Cross indicates the current operating point.

immediately after injection [6]. On the other hand, the lattice imperfections driving the half-integer resonance are assumed to have two components, namely, the time-dependent component ramping with the magnetic rigidity, which is supposed to mainly originate from the error field of main quadrupole magnets, and the time-independent component having a constant magnetic field. Thus, the perfect resonance compensation over the entire acceleration period of 20 ms is not achieved unless the time-dependent component of the lattice imperfections is taken into account.

To investigate the time-dependent component of the lattice imperfections, the resonance compensation during the later

stage of acceleration was explored. The timing of resonance-induced beam loss was arbitrarily controlled by adjusting the momentum offset and chromaticity-induced tune shift. The lattice imperfections were evaluated by the excitation currents of the QDTs required for the resonance compensation. Using an analysis based on the resonance drive term, we evaluated the optimal excitation pattern for the QDTs that maintains resonance compensation throughout the entire acceleration period.

EXPERIMENTS

To determine the time-dependent and -independent components of the lattice imperfections, we explored the resonance compensation by using the QDTs at a later stage of acceleration. For this purpose, it is necessary to be able to precisely control the timing at which the beam approaches the resonance within a range of a few milliseconds by adjusting the tune. Since such control by varying the strength of the quadrupole magnet is difficult, we utilized the chromaticity-induced tune shift and momentum offset generated by lowering the RF frequency. Figure 3 shows the momentum offset patterns numbered 1 through 11 employed in this study and the corresponding horizontal tunes calculated with the natural chromaticity of −9.1 of the RCS.

The experimental result employing the momentum offset is shown in Fig. 4. The beam was injected with an intensity of about 5 kw-eq. to ignore the space charge-induced tune spread and simplify the discussion. The momentum spread was also minimized to about 0.1%, mitigating the chromaticity-induced tune spread. Contrary to the vertical direction, the beam was injected with a large amplitude corresponding to the emittance of 200π mm·mrad, which reaches 62% of the collimator aperture, in the horizontal direction, to enhance the beam loss due to $2\nu_x = 13$ [3]. The beam loss was observed as the horizontal tune approached 6.5. Thus, the timing of the resonance-induced beam loss was well controlled by employing the momentum offset as expected.

To determine the time-dependent and -independent components of the lattice imperfections, the resonance compensation should be explored for each of the momentum offset patterns. The first part of our study was devoted to the pattern No. 7, in which the beam comes closest to $2\nu_x = 13$ at 9.3 ms after beam injection, since later timing of the beam loss is desirable to distinguish the time-dependent component from -independent component. Similarly, a beam loss of about several tens of percent is required to judge the resonance compensation. Figure 5 shows the time dependence of the beam survival rates related to the value at 5 ms. Each QDT was excited with a constant current of 30 A for 20 ms. The survival rates are clearly different depending on which QDT we excited. Considering that all QDTs are excited with the same current of 30 A and are arranged symmetrically in the RCS, the difference in beam survival rates indicates the excitation or compensation of the half-integer resonance. The beam survival rate was maximized by adding QDT1

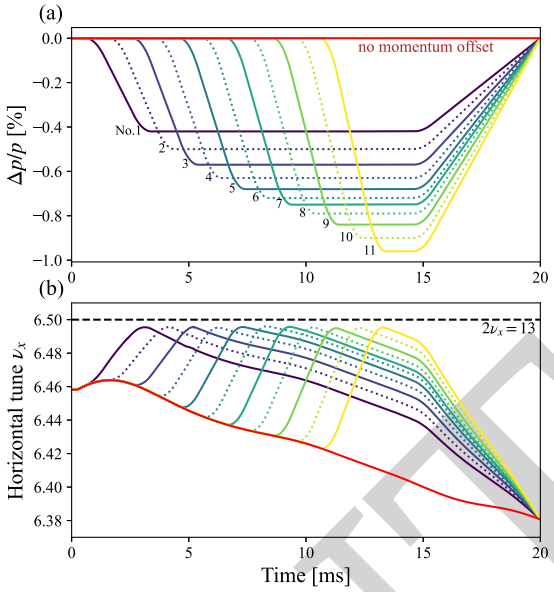

Figure 3: (a) Time evolution of the momentum offset and (b) corresponding horizontal tune are shown in solid and dotted curves. Black dashed line indicates the half-integer resonance condition.

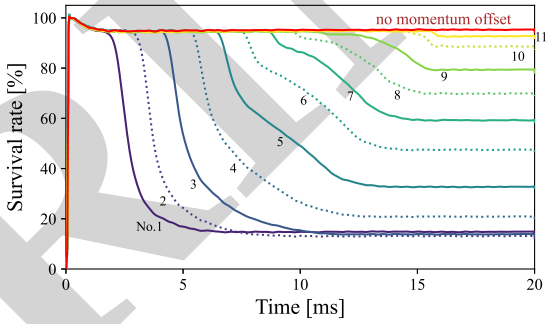

Figure 4: Time evolutions of beam survival rates measured by employing the momentum offset shown in Fig. 3 (a).

and QDT4 with the excitation currents of $I_1 = 20.0$ and $I_4 = 10.0$ A, respectively.

RESONANCE DRIVING TERM

A single particle Hamiltonian of the transverse motion subject to lattice imperfections can be written as

$$H(\phi_x, \phi_y, J_x, J_y; s) = \frac{J_x}{\beta_x} + \frac{J_y}{\beta_y} + \kappa_1(s)\beta_x J_x \cos^2\phi_x, \quad (1)$$

where s is the path length along the design beam orbit, κ_1 is s-dependent function representing the lattice imperfections, and $\beta_{x(y)}$ is the beta function. The resonance driving term (RDT) for the half-integer resonance is given by

$$\Delta G_{2,0,13} \approx \frac{1}{4\pi}\oint \beta_x(s)\kappa_1(s)e^{j[2\chi_x-(2\nu_x-13)\theta]}ds, \quad (2)$$

where j is imaginary. $\theta = 2\pi s/L$ is the scaled path length and L is the circumference of the RCS. In the general case,

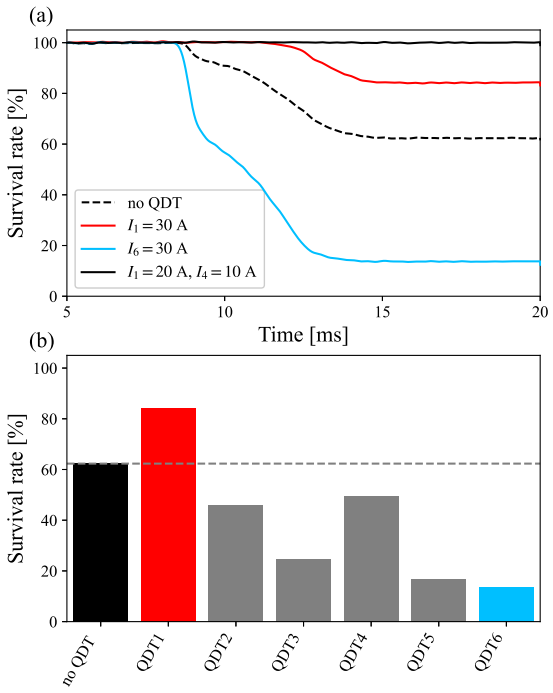

Figure 5: (a) Beam survival rates measured by employing the momentum offset pattern of No. 7 and (b) survival rates at 20 ms with an additional field generated by the QDTs independently excited with a current of 30 A. Unlike Fig. 4, the survival rate is scaled by the value at 5 ms.

$\kappa_1(s)$ is assumed to be composed of several error fields localized within a narrow area along the ring. Equation (2) is then approximated as

$$\Delta G_{2,0,13} \approx \frac{1}{4\pi} \sum_n \beta_x(s_n) K_{1,n} \times [\cos \Omega(s_n) + j \sin \Omega(s_n)],$$
$$\chi_x(s) = \int^s \frac{ds'}{\beta_x(s')}, \ \Omega(s) = 2\chi_x(s) - \frac{2\pi s}{L}(2\nu_x - 13), \quad (3)$$

where subscript n represents serial number of areas, and $K_{1,n}$ represents the strength of the error field in n-th area. The compensation of the half-integer resonance is equal to minimizing the RDT and can be achieved by the addition of QDTs to cancel out the lattice imperfections. As mentioned above, the lattice imperfections can be divided into two components, namely, the time-dependent and -independent components. Since the strength of the error field ramps proportionally to magnetic rigidity, $K_{1,n}$ of the time-dependent component is kept constant. Conversely, $K_{1,n}$ of the time-independent component is decreased inversely to magnetic rigidity.

The optimal excitation currents for QDT1 and QDT4 at 9.3 ms were found to be $I_1 = 20.0$ and $I_4 = 10.0$ A in the previous section. Similarly, the optimal excitation currents immediately after injection were found to be $I_1 = 26.6$ and $I_4 = 8.5$ A in previous studies [6]. Those excitation currents are assumed to generate the RDT opposite to that of lattice imperfections. The RDTs evaluated from the excitation currents for QDTs at 0 and 9.3 ms are shown in Fig 6. These RDTs direct different directions from each other due to the damping of K_1 of the time-independent component of the lattice imperfections. By comparing the RDTs, the time-dependent and -independent components are determined and indicated in blue and red lines, respectively. Moreover based on the RDTs, the half-integer resonance is expected to be successfully compensated by the addition of QDT1 and QDT4 with the excitation currents of $I_1(t) = 30.8\,\text{A} - 4.2\,\text{A}\,\frac{(B\rho)(t)}{(B\rho)(0)}$ and $I_4(t) = 6.5\,\text{A} + 2.0\,\text{A}\,\frac{(B\rho)(t)}{(B\rho)(0)}$ where t denotes time and $(B\rho)(t)$ is the magnetic rigidity at time t.

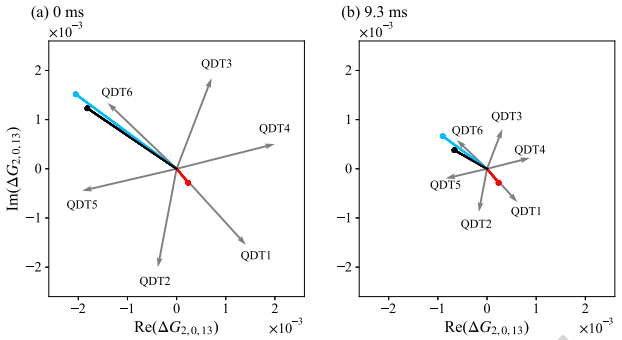

Figure 6: RDTs at (a) 0 and (b) 9.3 ms after beam injection. Gray arrows indicate the RDTs of each QDT excited with a current of 30 A. Black line indicates the RDTs generated by the lattice imperfections, and their time-dependent and -independent components are shown in red and blue lines, respectively.

SUMMARY

To enhance the tunability of the operating point for beam power ramp-up, the compensation of the half-integer resonance was experimentally studied. The timing at which the beam approaches the resonance was arbitrarily controlled by utilizing the chromaticity-induced tune shift. The excitation currents for QDTs canceling out the lattice imperfections at 9.3 ms after beam injection were found to be $I_1 = 20.0$ and $I_4 = 10.0$ A, and the RDT of lattice imperfections is evaluated. By comparing the RDTs at 0 and 9.3 ms, the RDTs of the time-dependent and -independent components were evaluated. In addition, the excitation pattern of QDTs expected to achieve compensation for the half-integer resonance for the entire acceleration period of 20 ms was evaluated. In the near future, the resonance compensation will be explored similarly for the other momentum offset patterns, and the excitation pattern of QDTs will be refined. Subsequently, our resonance compensation will be verified for high-intensity beams.

REFERENCES

[1] Accelerator Group, JAERI/KEK Joint Project Team, "Accelerator technical design report for high-intensity proton accelerator facility project, J-PARC", 2003. https://cds.cern.ch/record/74720

[2] P.K. Saha *et al.*, "State-of-the-art beam loss minimization at high-intensity beam operation of the 3 GeV rapid cycling synchrotron at the Japan Proton Accelerator Research Complex",*Phys. Rev. Accel. Beams*, vol. 28, p. 074201, 2025. doi:10.1103/tbyh-jcq3

[3] H. Harada, "Painting-injection study using a virtual accelerator in a high-intensity proton accelerator", Ph.D thesis of Hiroshima University, 2009.

[4] P.K. Saha *et al.*, "Direct observation of the phase space footprint of a painting injection in the Rapid Cycling Synchrotron at the Japan Proton Accelerator Research Complex", *Phys. Rev. ST Accel. Beams*, vol. 12, p. 040403, 2009. doi:10.1103/PhysRevSTAB.12.040403

[5] H. Hotchi *et al.*, "Beam commissioning and operation of the Japan Proton Accelerator Research Complex 3-GeV rapid cycling synchrotron", *Prog. Theor. Exp. Phys*. vol. 2012, pp. 2B003-0, 2012. doi:10.1093/ptep/pts021

[6] K. Kojima *et al.*, "Half-Integer Random Resonance Compensation for Further Beam Power Ramp-up in the 3-GeV Rapid Cycling Synchrotron of the Japan Proton Accelerator Research Complex", *Prog. Theor. Exp. Phys.*, vol. 2025, p. 013G01, 2024. doi:10.1093/ptep/ptae185